Image-Based Validation of Optically Coupled Current Sensor for RF Safety Monitoring

Maryam Etezadi-Amoli[1], Pascal Stang[1], Adam Kerr[1], John Pauly[1], and Greig Scott[1]
[1]*Electrical Engineering, Stanford University, Stanford, CA, United States*

Introduction: The RF transmit fields in MRI can induce currents in long conductors, which can then lead to dangerous heating of surrounding tissues. This safety hazard presents challenges for interventional MRI, where guidewires and ablation catheters are often made of conductive material, and it also precludes patients with implanted medical devices such as pacemakers and neurostimulators from receiving MRI scans. The ability to quantitatively monitor induced RF currents in real time during an MRI scan could greatly increase the safety of such scans and lead to a better understanding of the coupling mechanisms between medical devices and transmit fields.

Zanchi et al. [1] presented a toroidal current sensor that could measure the magnitude and phase of induced wire currents. Recently, this sensor was modified (Fig. 1) to use a photonic power supply instead of a battery in order to eliminate all magnetic components and allow the sensor to be placed close to the imaging volume without causing susceptibility artifacts. The new sensor also contains additional shielding to prevent ambient fields from confounding the wire current measurements [2]. In this work, we validate the accuracy of this sensor by comparing both submerged and free space current sensor measurements to current computed from B1 maps within the imaging volume.

Methods: To calibrate the sensor, we connected a measured load consisting of a wire loop and resistor to a function generator with known output impedance and open circuit voltage characteristic. This allowed us to induce a known amount of RF current on the wire and measure the corresponding sensor output.

An EP catheter model (~9F insulated wire with 5mm of exposed conductor at wire tip) was then inserted in a saline gel phantom as shown in Fig. 4. The current sensor was moved to different wire locations both outside the phantom and submerged in the phantom in order to map the wire current. A transmit-receive toroid [3] was used to acquire axial Bloch-Siegert B1 maps [4] (1.5T, TR/TE = 50/6ms, 256x256, 12cm FOV) at various slice locations close to each current sensor location. Corrections were made for image distortion caused by gradient nonlinearities for slices away from isocenter, and the wire current was computed from the B1 map by performing a least squares fit to the equation $|B1^+| = \mu_0 I/(4\pi r)$. The image-derived current values were compared to the current sensor readings to assess the accuracy of the current sensor.

Results: Figure 3 shows the image-based current computation for one of the wire locations. A disk shaped region is used for current computation to avoid low SNR B1 values far away from the wire and values near the wire center that may have phase-wrapping errors. There is less than 10% error between current sensor measurements and current values computed from co-located B1 maps (Fig. 4), which is a very reasonable error margin considering the possible sources of inaccuracies such as errors in the calibration procedure, noise in the B1 maps, and thermal and temporal drift in amplifiers and power supplies.

Discussion: In Fig. 4, we see that the current inside the body can be higher than outside the body, and thus a single measurement outside the body may not suffice to fully characterize the current pattern on the immersed wire segment. Possible extensions include using multiple current sensors outside the body or developing a single sensor that measures both electric and magnetic field.

Conclusion: We have shown very good agreement between current sensor measurements and image-based current computation. These measurement methods can be essential tools for RF safety in interventional scenarios where we have access to the implant, and in the case of fully implanted medical devices.

References: [1] Zanchi et al., IEEE Trans. Med. Imag. 29:169-178, 2010. [2] Etezadi-Amoli et al., ISMRM Workshop on MR Safety in Practice, Lund Sweden, 2012. [3] Etezadi-Amoli et al., Proc. 19th ISMRM, p1749, 2011. [4] Sacolick et al., MRM 63:1315-1322, 2010. NIH grant support: R01EB008108, R33CA118276, P01CA159992.

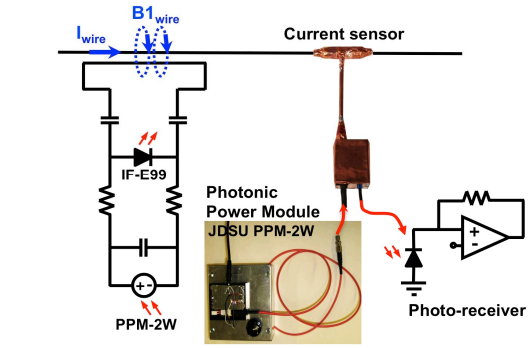

Figure 1: The toroidal cavity of the current sensor acts as a pick-up loop for B1 fields associated with RF wire currents. An optical fiber from the photonic power module supplies bias power to the IF-E99 LED, and a separate optical fiber transmits the LED light to a photo-receiver stage [2].

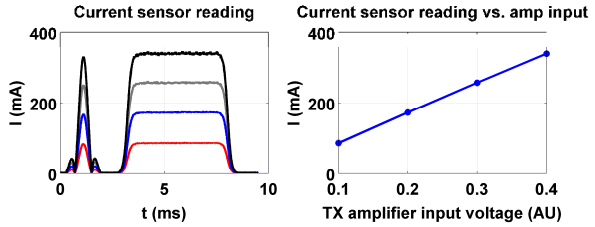

Figure 2: Left: Current sensor measurements when transmitting with 4 different amplitudes of Bloch-Siegert B1 mapping pulses [4]. Right: The sensor exhibits good linearity: peak current magnitude increases proportionally to the transmit amplifier input voltage.

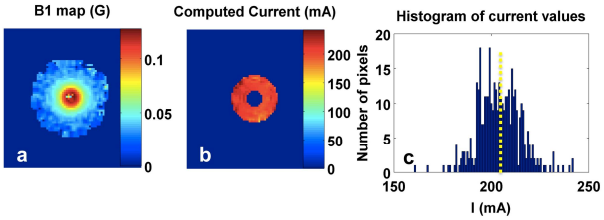

Figure 3: (a) Axial B1 map, (b) disk-shaped mask region and computed current, (c) histogram of current values with least squares fit value shown by dotted yellow line.

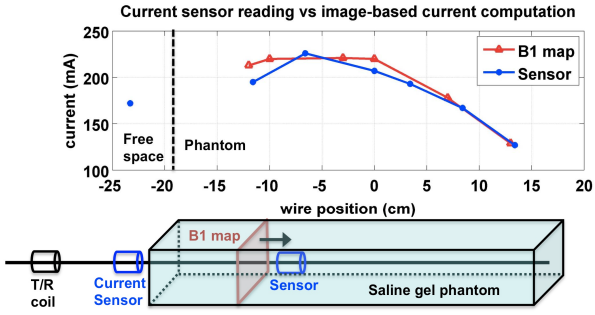

Figure 4: Comparison of sensor measurements and current computed from B1 maps at various slice locations. Sensor measurements differ from B1-map computed current by < 10% for sensor and slice locations within 5cm of each other. Interestingly, the wire current can be higher inside the phantom than outside, as shown by the free space measurement of 172mA outside the phantom, compared to a peak value of 220mA inside the phantom.